Since January 2020 Elsevier has created a COVID-19 resource centre with free information in English and Mandarin on the novel coronavirus COVID-19. The COVID-19 resource centre is hosted on Elsevier Connect, the company's public news and information website.

International Journal of Infectious Diseases 99 (2020) 505–513

Contents lists available at ScienceDirect

International Journal of Infectious Diseases

journal homepage: www.elsevier.com/locate/ijid

A fluid mechanics explanation of the effectiveness of common materials for respiratory masks

Blake Maher[a,b], Reynaldo Chavez[a,b], Gabriel C.Q. Tomaz[a,c], Thien Nguyen[a,c,*], Yassin Hassan[a,b,c]

[a] Thermal-Hydraulic Research Laboratory, Texas A& M University, College Station, Texas 77843, USA
[b] J. Mike Walker' 66 Department of Mechanical Engineering, Texas A& M University, College Station, Texas 77843, USA
[c] Department of Nuclear Engineering, Texas A& M University, College Station, Texas 77843, USA

ARTICLE INFO

Article history:
Received 28 May 2020
Received in revised form 22 July 2020
Accepted 26 July 2020

Keywords:
COVID-19
Face masks
Respiratory masks
Filtration efficiency
Aerosol droplets
Flowfield characteristics
Household materials
Pressure difference

ABSTRACT

Objectives: Face masks are an important component of personal protection equipment employed in preventing the spread of diseases such as COVID-19. As the supply of mass-produced masks has decreased, the use of homemade masks has become more prevalent. It is important to quantify the effectiveness of different types of materials to provide useful information, which should be considered for homemade masks.

Methods: Filtration effects of different types of common materials were studied by measuring the aerosol droplet concentrations in the upstream and downstream regions. Flow-field characteristics of surrounding regions of tested materials were investigated using a laser-diagnostics technique, i.e., particle image velocimetry. The pressure difference across the tested materials was measured.

Results: Measured aerosol concentrations indicated a breakup of large-size particles into smaller particles. Tested materials had higher filtration efficiency for large particles. Single-layer materials were less efficient, but they had a low pressure-drop. Multilayer materials could produce greater filtering efficiency with an increased pressure drop, which is an indicator of comfort level and breathability. The obtained flow-fields indicated a flow disruption downstream of the tested materials as the velocity magnitude noticeably decreased.

Conclusions: The obtained results provide an insight into flow-field characteristics and filtration efficiency of different types of household materials commonly used for homemade masks. This study allows comparison with mass-produced masks under consistent test conditions while employing several well-established techniques.

Introduction

The use of face masks has been widely accepted as the first personal protection during the COVID-19 pandemic because the transmission of the respiratory virus is mainly via human laden fluid particles, i.e., aerosols and droplets (Konda et al., 2020; Mittal et al., 2020; Kutter et al., 2018; Stelzer-Braid et al., 2009; Milton et al., 2013). In addition to maintaining a social distance and constantly washing hands with soap, wearing personal face masks can provide an immediate solution to individuals who may live and/or work in areas such as public offices, supermarkets, hospitals, buildings, and train stations, with a high risk of being exposed to the respiratory virus. Many studies have attempted to characterize respiratory aerosol droplet characteristics such as density, velocity, and size distributions (Wells, 1934; Duguid, 1946; Wells, 1955; Morawska et al., 2009; Xie et al., 2009; Han et al., 2013; Bourouiba et al., 2014; Scharfman et al., 2016; Asadi et al., 2019). Measured droplet sizes can vary a few orders of magnitude, i.e., $\boldsymbol{O}(0.1)$ to $\boldsymbol{O}(1000)$ μm (Mittal et al., 2020). While large size droplets may settle before evaporating and deposit on surrounding surfaces, small and medium-sized droplets evaporate and form droplet nuclei that may stay airborne or be suspended for many hours.

The filtration of aerosol droplets using a face mask is governed by these basic mechanisms: impaction, gravity sedimentation, interception, diffusion, and electrostatic attraction (Hinds, 1999; Vincent, 2007; Konda et al., 2020; Mittal et al., 2020). The

* Corresponding author at: Thermal-Hydraulic Research Laboratory, Texas A&M University, College Station, Texas 77843, USA.
E-mail address: thien.duy.ng@tamu.edu (T. Nguyen).

https://doi.org/10.1016/j.ijid.2020.07.066

contribution of each mechanism to the filtration effects of a face mask depends on the materials used, aerosol droplet sizes, and the relative conditions (temperature, humidity, and air velocity) of the considered areas. For aerosol droplets ranging from ~ 1 μm–10 μm, sedimentation, impaction, and interception mechanisms are more important (Rostami, 2009). For small particles as droplet-nuclei-sized particles, i.e., less than 1 μm, diffusion by Brownian motion and interception of particles by the filter fibers are the dominant mechanisms (Konda et al., 2020). Electrostatic attraction is important to catch the nanometer-sized particles, which can penetrate through the holes in the material structures.

The droplet nuclei may have a significant travel distance depending on the ambient air currents and indoor environments and the cabins of transportation vehicles (Bourouiba et al., 2014). In these spaces, the presence of circulation flows by ventilation systems, the open/close mechanisms of doors, and their effects on the airborne transmission of the respiratory virus are important and should be carefully considered (Tang et al., 2006; Li et al., 2007; Craven and Settles, 2006; MacIntyre et al., 2008; Licina et al., 2014; Offeddua et al., 2016). Personal face masks can be considered as physical barriers; using face masks in public areas could retard the transmission of respiratory infections (Barasheed et al., 2016; Mittal et al., 2020). The increase in demand and reduction in supplies of commercial masks have brought the option of do-it-yourself (DIY) or homemade masks to be a practical and feasible solution. Homemade masks usually consist of various household materials such as synthetic and natural cloths (non-woven fabric and cotton), microfiber cloths, and households filtering materials, for example, HVAC filters, coffee filters, and vacuum bags (Chughtai et al., 2014; Konda et al., 2020). It is essential to acquire a proper understanding of the effects of commonly used materials for DIY face masks such as the filtration efficiency and the effects of face masks in surrounding flow-fields.

The focus of the present study is to investigate the aerosol filtration efficiency of common household materials and their effects on flow characteristics in the surrounding flow regions. The flow field characteristics in the upstream and downstream regions of tested materials are obtained using a laser-diagnostics approach, i.e., the particle image velocimetry (PIV) technique. This study utilized an isokinetic sampling probe to collect a small volume of aerosol droplets for analysis. Note that the velocity chosen in this study was within the range of airflow velocities that are commonly found in indoor public areas, such as homes, offices, supermarkets, airplanes, trains, and buses, where the air flows are circulated by ventilation systems. Characterizing the effectiveness of respiratory masks with respect to the airborne transmission by the air flows within these areas is important. The conditions tested in this study are different compared to coughing or regular breathing such that the air velocity generated by a cough versus regular breathing is not continuous. The maximum velocities of human breathing and coughing could be approximately 10 m/s and 16 m/s, respectively. Recent experimental, numerical, and modeling studies can be found in Busco et al. (2020) for the dynamics of human sneezing and asymptomatic respiratory virus transmission, and in Dbouk and Drikakis (2020a, b) for the penetration and travel distances of airborne droplets through a face mask.

Materials, experimental facility, and measurement techniques

We studied the filtration efficiency of common household materials, such as cotton, non-woven fabric (fabric 1), microfiber cloth, HVAC filter, shower curtain, vacuum bag, and coffee filter, made up as either a single-layer, two-layers, or three-layers, and compared them to a commercial surgical mask and an R95 mask (see Table 1).

Figure 1 shows an overview of the experimental apparatus that was constructed to study the effects of materials on flow behavior. The apparatus had a cross-sectional area of 7.62 × 7.62 cm^2 and a total length of 182.88 cm. It was divided into three equal sections; each had a 60.96 cm length, connected using flanges. The test materials were placed in between the second and the third sections. A volumetric air flow rate of 300 LPM, measured by a rotameter, was maintained for all the measurements. The resulting air velocity in the upstream region of the tested materials was 0.86 m/s, which is within the range of air velocity inside public areas, such as offices and buildings, generated by a ventilation system. Differential pressures (ΔP) across the tested materials, indicating the comfort level and breathability of a person when putting on the face masks, were measured using a Dwyer manometer with a reading accuracy of 0.02 inch of water (~4.97 Pa).

To generate the liquid aerosol droplets, a six jet-atomizer (TSI Model 9306) was used to aerosolize the Di-Ethyl-Hexyl-Sebacat (DEHS) fluid. The generated liquid droplets had a mean diameter of 1 μm and a density of 910 kg/m^3. The aerosol droplet size and density are chosen to represent the common properties of airborne particles that are often considered more harmful than larger-size particles because of their ability to penetrate human bronchi and lungs (Shakya et al., 2017). To acquire the aerodynamic flow fields in the upstream and downstream regions of the tested materials, two-dimensional two-component (2D2C) PIV measurements were performed. The 2D2C PIV system consisted of a 20 W continuous laser with a green wavelength of 527 nm and a high-speed CMOS Phantom M310 camera. For each flow measurement of the tested materials, the camera operated in a single-frame mode and captured a sequence of 8341 images of 1280 × 1280 pixels at a frequency of 500 Hz. The collection of PIV experimental images

Table 1
Averaged filtration efficiency and pressure differences of single-layer and multi-layer materials tested in this study.

Materials	Averaged Filtration Efficiency	ΔP (Pa)
Cotton (Original / Washed)	87% / 85%	74.7
Non-woven Fabric (Fabric 1) (Original / Washed)	83% / 79%	29.9
Micro Fiber Cloth (Original / Washed)	83% / 83%	44.8
HVAC Filter	74.7%	64.8
Shower Curtain	74.4%	64.7
Vacuum Bag	95.2%	478.2
Surgical Mask	81.4%	378.6
Mask R95 (Original / Washed)	99% / 96%	169.4
Cotton – Cotton	91%	296.4
Cotton - HVAC	90%	211.7
Cotton – Fabric 1	91%	214.2
Cotton – Coffee Filter	91%	473
Cotton – Coffee Filter - Cotton	92%	548
Cotton – Coffee Filter – Fabric 1	91%	403.5

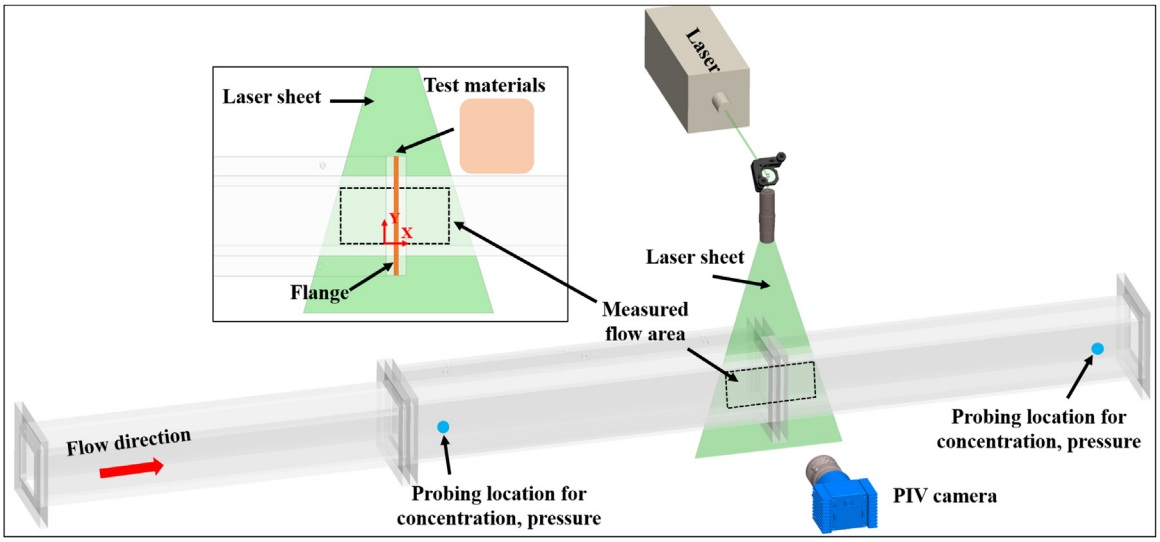

Figure 1. Experimental setup to measure the flow-fields, aerosol droplet concentrations, and pressure difference across the materials.

was processed using in-house codes (Eckstein and Vlachos, 2009; Nguyen et al., 2017; Nguyen and Hassan, 2017; Nguyen et al., 2018a; Nguyen et al., 2018b; Nguyen et al., 2019a; Nguyen et al., 2019b; Nguyen et al., 2019c; Nguyen et al., 2020). The estimated overall uncertainty of the PIV processing code was approximately 0.1 pixels, yielding less than 1% of the mean centerline velocity of the upstream region.

The particle concentrations at the upstream and downstream locations of the tested materials were measured utilizing an isokinetic sampling probe, which collected a small volume of aerosol droplets for flow analysis. The spatial distances from the tested materials to the upstream and downstream sampling locations of OPS were 520 mm and 470 mm, respectively. For each tested material, ten experimental runs to obtain particle concentrations were performed for each sampling location; each run was recorded with a duration of 1 minute.

A high magnification imaging system was utilized to capture images of tested materials' surfaces. The imaging system consisted of an 8-MP CCD camera (Imperx B3320) with a maximum resolution of 2458 × 3312 pixels, and a 12X zoom lens with a 3-mm fine focus (ThorLabs MVL12 × 3Z). The scaling factor between image pixel to physical dimension (μm) is 8:10. High-resolution images taken on the surfaces of tested materials are provided in Figure 2.

Results and discussions

Results from flow-field measurements

Figure 3 illustrates the normalized mean velocity fields obtained from PIV measurements for the upstream and downstream regions of the tested materials. Results corresponding to the case without materials, named the based case, are also included in Figure 3. Velocity vectors are the normalized horizontal, U/U_m, and vertical, V/U_m, velocity components, while the color represents the normalized velocity magnitude, $|U|/Um = \sqrt{U^2 + V^2}/U_m$. Here, U_m is selected as the mean centerline velocity at the location (x,y) = (-30, 38.1) mm.

Flow-fields in the upstream region of the tested materials are similar to that of the based case, while flow patterns in the downstream region are altered and different among the tested materials. Also, color maps of the normalized velocity magnitude $|U|/Um$ depict significant reductions in the downstream region. Notably, the downstream region of the tested mask R95 has a very small velocity magnitude.

Figure 4 compares the probability distributions of normalized velocity magnitudes extracted from the upstream and downstream regions. In these plots, the normalized velocity magnitudes $|U|/Um$ are distributed in the 20 bins ranging from 0 to 1 with an equal bin width of 0.05. The probability distributions computed for the upstream region of tested materials are almost similar to that of the base case, while the probability distributions obtained for the downstream region of tested materials are different compared to the base case. Probability distributions in Figure 4 confirmed the significant reduction of velocity magnitude in the downstream region observed in Figure 3 of the mean velocity fields.

Results from aerosol droplet concentration measurements

In this section, results obtained from measurements of aerosol droplet concentrations and pressure differences across the tested materials are presented. The filtration efficiency per aerosol droplet size, FE_{D_i}, is defined as

$$FE_{D_i} = \frac{C_{u,D_i} - C_{d,D_i}}{C_{u,D_i}} \quad (1)$$

where D_i is the aerosol diameter at bin i^{th}, C_{u,D_i}, and C_{d,D_i} are the concentrations measured at the upstream and downstream locations, respectively. If the computed filtration efficiency was below 0, i.e., when $C_{u,D_i} < C_{d,D_i}$, the negative FE values were removed from the result presentations and further calculations. The averaged filtration efficiency is computed using the filtration efficiency weighted by the mass of aerosol droplets of various bins. It is expressed as

$$FE_{ave} = \frac{FE_{D_i} \cdot m_{D_i}}{\sum m_{D_i}} \quad (2)$$

where m_{D_i} is the mass of aerosol droplet computed for bin i^{th}.

Figure 5 shows the results of aerosol droplet concentrations measured at the upstream, C_u, and downstream, C_d, locations of the tested materials as a function of particle sizes. Results were obtained at the flow rate of 300 LPM and for different types of materials, including single-layer, two-layers, and combined multi-layers of various materials. Table 1 summarizes the averaged filtration efficiency and measured pressure differences between

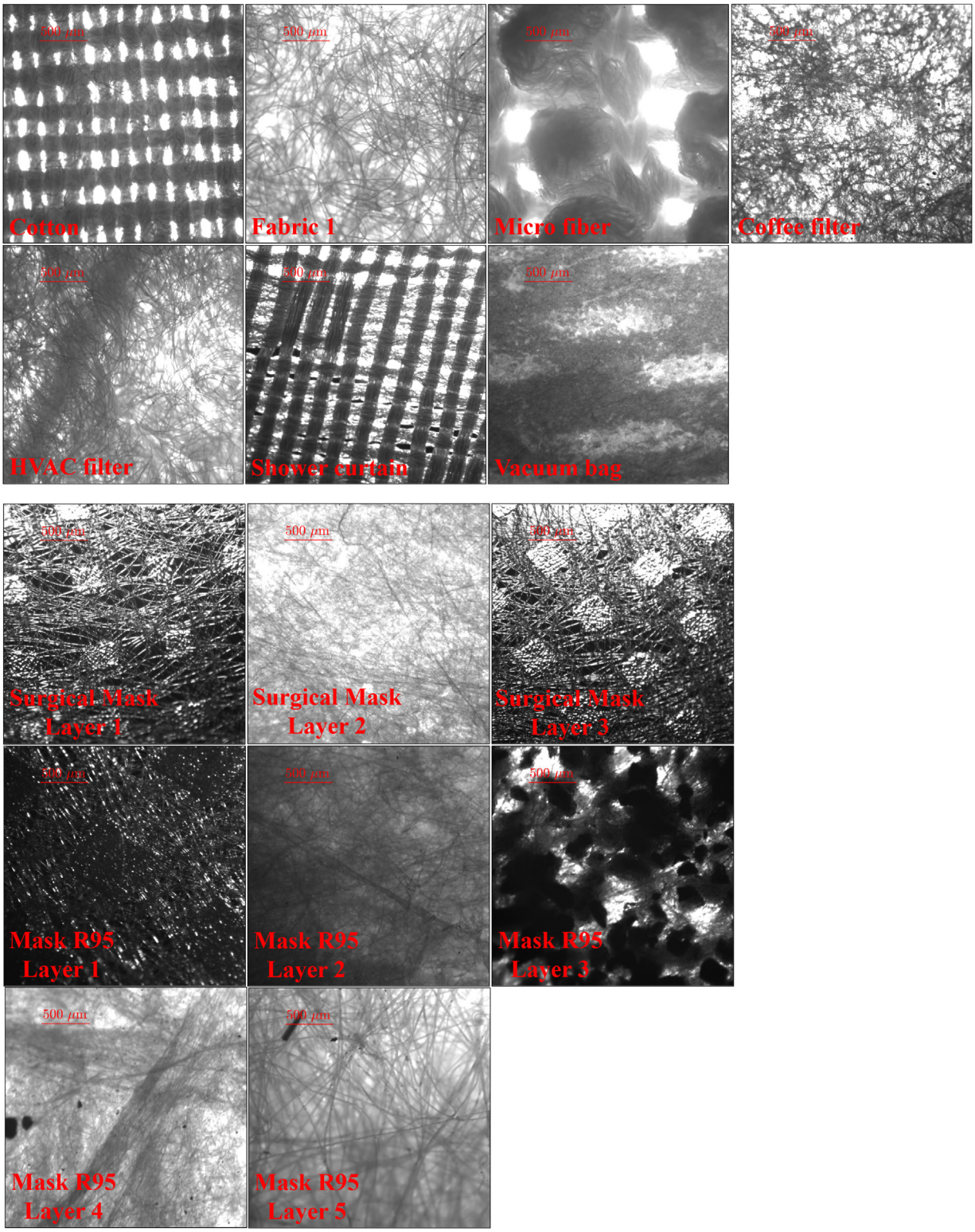

Figure 2. High-resolution images of tested materials, i.e., cotton, fabric 1, microfiber, coffee filter, HVAC filter, shower curtain, and vacuum bag. Images of commercial surgical mask (three layers) and R95 mask (five layers) are also included. Scale bar shown is 500 μm and the size of images presented is 2.5 × 2.5 mm^2.

the upstream and downstream locations for various materials tested in this study. In Figure 5, aerosol concentrations measured by the OPS at the upstream location of tested materials showed high values for aerosol sizes ranging from 1 μm to 4.7 μm. This range of aerosol droplet diameters matched well with the performance characteristics provided by the manufacturer for the aerosol droplet generator used in this study.

For all tested materials, within the aerosol sizes from 1 μm to 4.7 μm, the measured aerosol concentrations at the downstream location were reduced, indicating the filtration effects of the

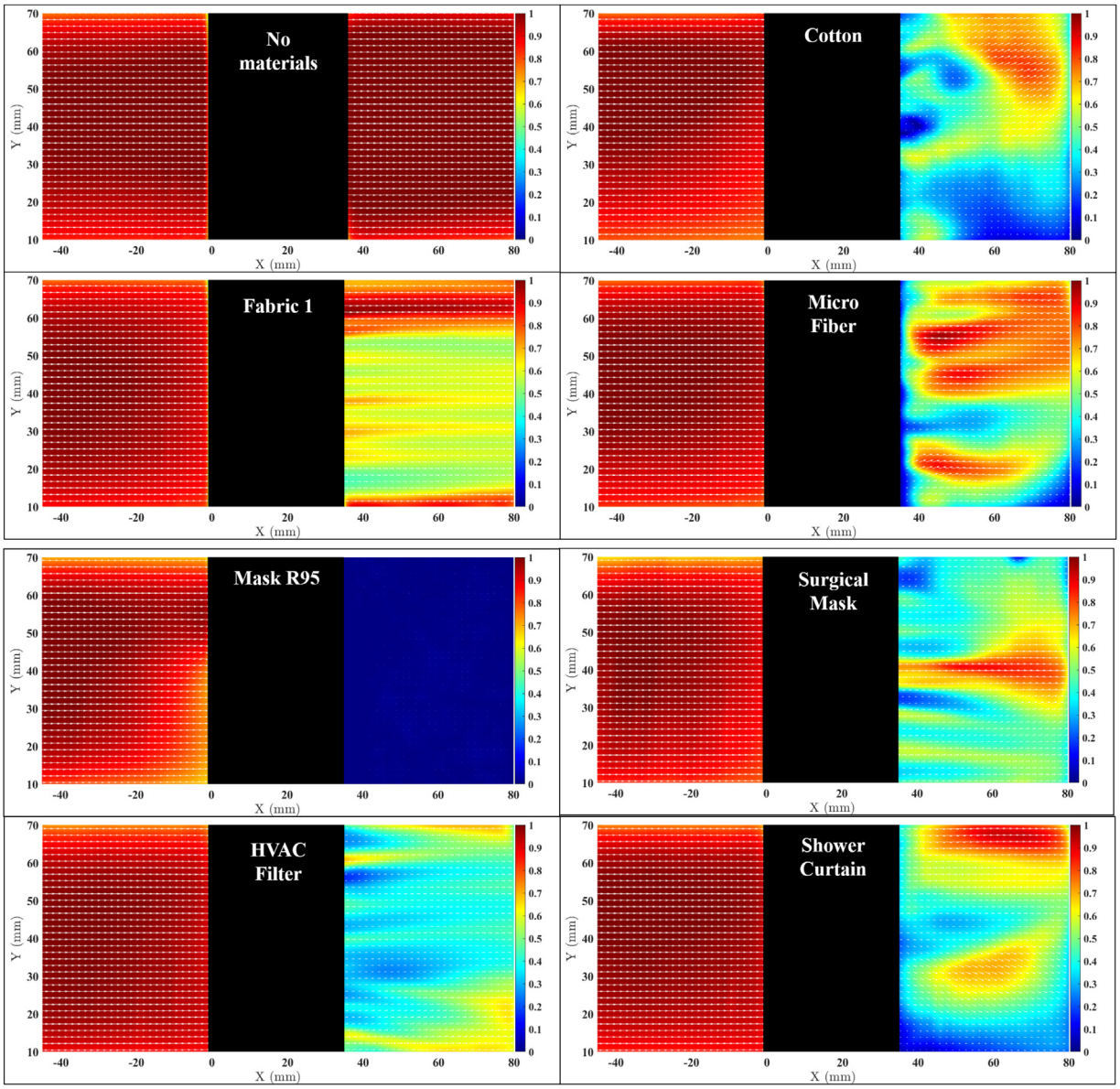

Figure 3. Results from flow-field measurements in the upstream and downstream regions of the test section for various materials. Presented results are normalized mean in-plane velocity vector fields, U/Um and V/Um, and color contours of normalized mean velocity magnitude, $|U|/Um$.

studied materials. For the concentration measurements of aerosol sizes smaller than 0.7 μm, Figure 5 shows that aerosol concentrations increased and mainly distributed within the aerosol sizes ranging from 0.38 μm to 0.52 μm. Such observations could be explained by the fact that when aerosol droplets with large diameters impinged onto the front side of tested materials, they broke into smaller droplets and passed through the layer. In this circumstance, characteristics of aerosol droplets, such as sizes and concentrations, measured at the downstream location, will depend on the porosity of tested materials. Among the tested materials as a single layer, the cotton, fabric 1, and microfiber cloth have nearly similar concentrations of aerosol droplets larger than 1 μm measured at the downstream location. Figure 5, it was found that the filtration effects of tested materials increased as combined layers increased, when compared to the filtration effects of single-layer materials.

Figure 6 depicts the filtration efficiency of various materials that were tested as a single layer, i.e., cotton, fabric 1, microfiber, HVAC filter, and shower curtain, and as multiple layers, i.e., vacuum bag, surgical mask, mask R95, cotton-cotton, cotton-fabric 1, cotton-HVAC filter, cotton-coffee filter, cotton-coffee filter-cotton, and cotton-coffee filter-fabric 1. In Figure 6, the computed filtration efficiency FE_{D_i} is presented per aerosol droplet size D_i ranging from 1 μm to 4.67 μm. In comparisons of filtration efficiency computed for materials tested as a single layer, it can be seen that the shower curtain and HVAC filter had lower efficiency for all aerosol droplets sizes and their averaged filtration efficiency was 74.4% and 74.7%, respectively. Cotton, fabric 1, and microfiber had their filtration efficiency greater than 92% for aerosol droplets with sizes from 2.42 μm and higher, and the averaged filtration efficiency was 87%, 83%, and 83%, respectively. Figure 6 (bottom) shows that the use of multilayer materials combining cotton, fabric 1, HVAC filter, and coffee filter improved the filtration efficiency for all aerosol droplet sizes. Moreover, as can be observed in Table 1, the averaged filtration efficiency of the combined multilayer materials increased from 4% to 15% when compared to those of the single-layer materials. It is important to note that at the aerosol droplet size of 2.42 μm, all the tested multilayer materials had

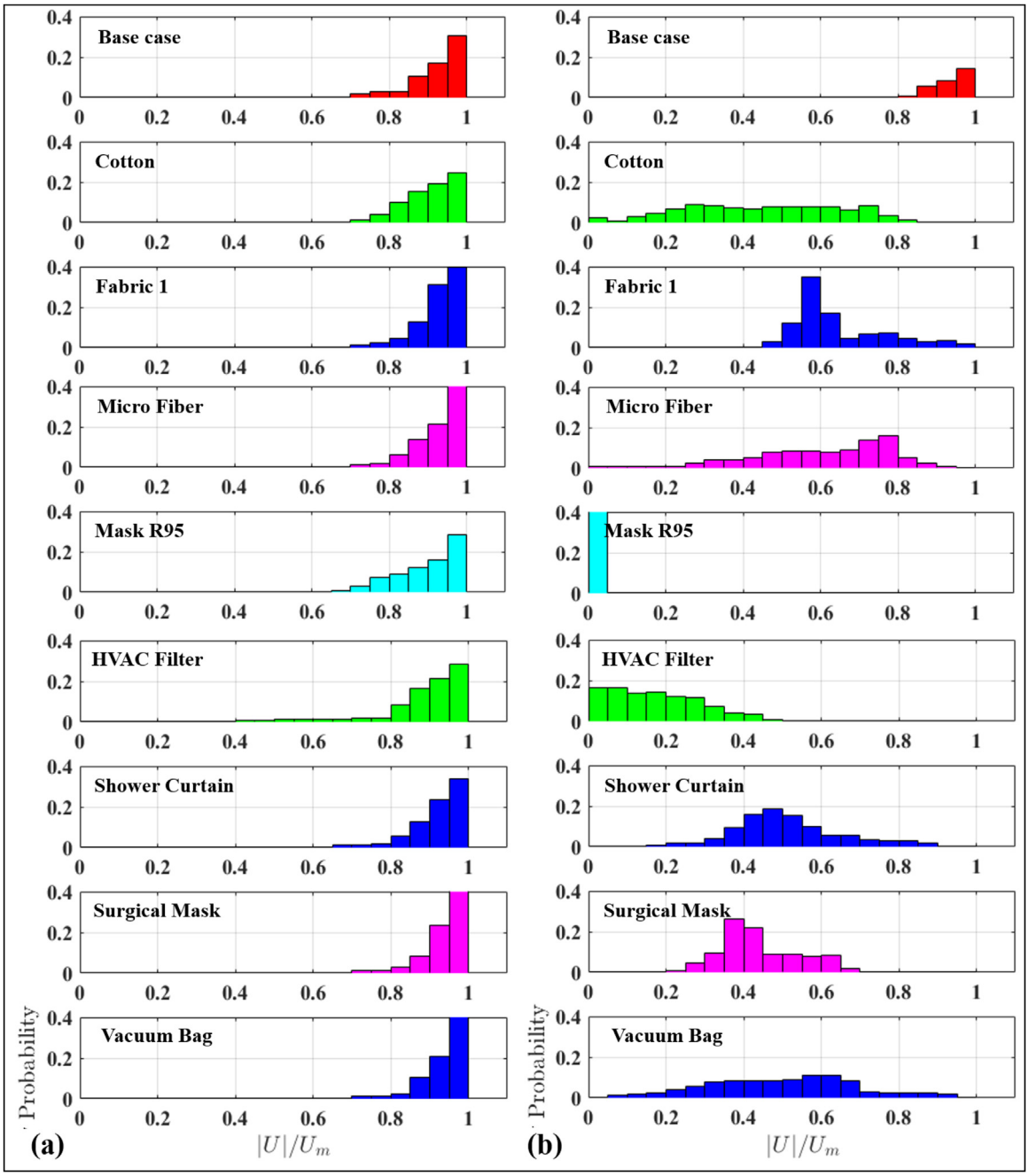

Figure 4. Probability distributions of normalized velocity magnitude extracted from the (a) upstream and (b) downstream regions of the base case (no material) and tested materials, including cotton, fabric 1, micro fiber, mask R95, HVAC filter, shower curtain, surgical mask, and vacuum bag.

their filtration efficiency greater than 95%. Results presented in Figure 6 and Table 1 also included the filtration efficiency computed for the commercial surgical mask with three layers and an R95 mask with five layers. It is observed that surgical masks had lower filtration efficiency than the cotton-cotton at droplet sizes of 1 μm and 1.25 μm. However, for aerosol droplets with sizes greater than 2.42 μm, the filtration efficiency of the surgical mask increased significantly to greater than 95%. The tested R95 mask had very high filtration efficiency for all the aerosol droplet sizes, i.e., 93.4% at 1 μm and greater than 95% for droplet sizes larger than 1.25 μm. The averaged filtration efficiency of the surgical mask and R95 mask was 81.4% and 99%, respectively.

The measured pressure differences across the tested materials provided in Table 1 could be used as an indicator for the level of comfort and breathability when the materials are used for face masks. For the single-layer materials, non-woven fabric 1 had the smallest pressure difference (29.9 Pa) due to its porous structure, while cotton had the highest pressure drop of 74.7 Pa. Pressure differences of the two-layer materials increased approximately three to four times higher than those of the single-layer ones. It is interesting to see that the tested vacuum bag (two layers) also had a significant averaged filtration efficiency of 95.2%. However, its pressure difference of 478 Pa is significant compared to other two-layer materials, indicating the low-level of comfort and

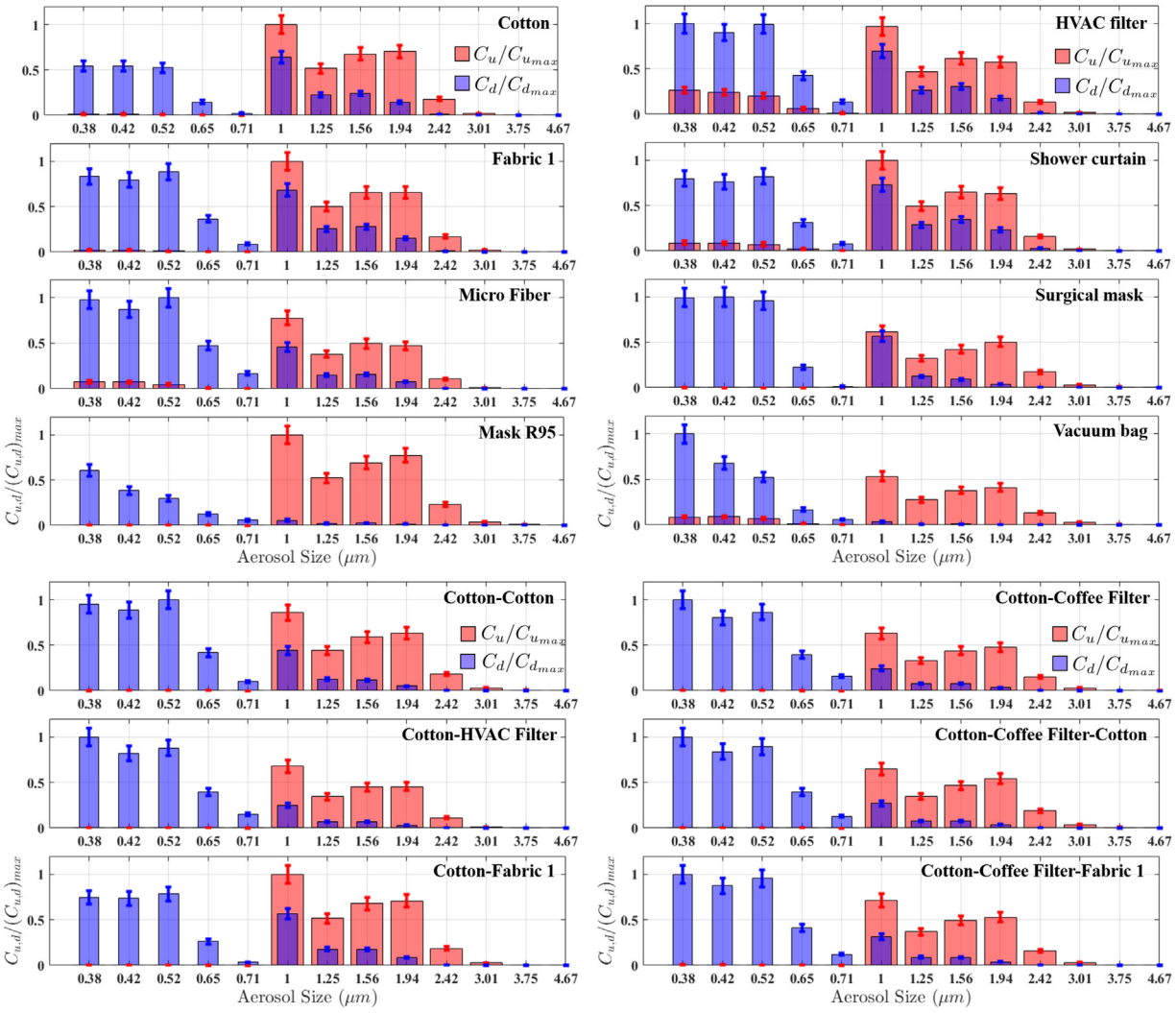

Figure 5. Aerosol concentrations measured at the upstream, *Cu*, and downstream, *Cd*, locations of the tested materials as a function of aerosol sizes and at the flow rate of 300 LPM. Each bin shows the particle concentration averaged over ten trials.

breathability if used as a face mask. The combinations of a cotton-HVAC filter and cotton-fabric 1 had the smallest pressure difference of 211.7 Pa and 214.2 Pa, respectively, and similar averaged filtration efficiency. Results presented in Table 1 indicate that the use of cotton-coffee filter material had an averaged filtration efficiency of 91% but a high-pressure difference of 473 Pa, i.e., more than two times greater than that of cotton-fabric 1. The filtration effects of single-layer materials, i.e., cotton, fabric 1, and microfiber, were also tested after they were washed using a washer for 20 min. The same process of concentration measurements at the upstream and downstream locations was performed on the washed materials. Results shown in Table 1 indicate that the averaged filtration efficiency of cotton, fabric 1, and microfiber reduced around 2%–4% after being washed in a washer.

Among the three-layer materials tested in this study, the cotton-coffee filter-cotton, and cotton-coffee filter-fabric 1 had their filtration efficiency higher than 90%. Although the surgical mask had an averaged filtration efficiency of 81.4%, its pressure difference of 378.6 Pa was the smallest one among all three-layer materials. The tested R95 mask (five layers) had a pressure difference of 169.4 Pa, which was even lower than those of the two-layer materials. This could be explained by the fact that the five layers of the R95 mask were porous, yielding small pressure drop values.

Summary

The focus of this study was to investigate the filtration effects of various materials that are commonly available in households and stores and have been considered for DIY or homemade respiratory masks. The filtration efficiency of single-layer and multilayer materials were characterized for aerosol particles ranging from 0.3 μm to 6 μm; this range is within that of the aerosol-based virus transmission. Also, the flow-field characteristics in the upstream and downstream regions of the tested materials were experimentally acquired to visualize the effects of materials on the flow.

It was found that the flow-fields in the downstream region were altered by the presence of the tested materials, such that the velocity magnitude was significantly reduced. The probability distributions of velocity magnitudes computed for the upstream region of the tested materials were almost similar to that of the base case, i.e., flow-fields experimentally obtained without the tested materials. On the other hand, the probability distributions of velocity magnitudes computed for the downstream region were different from the base case, confirming the velocity reduction observed in the velocity flow fields.

All tested materials provided filtration effects to aerosol droplets within the size from 1 to

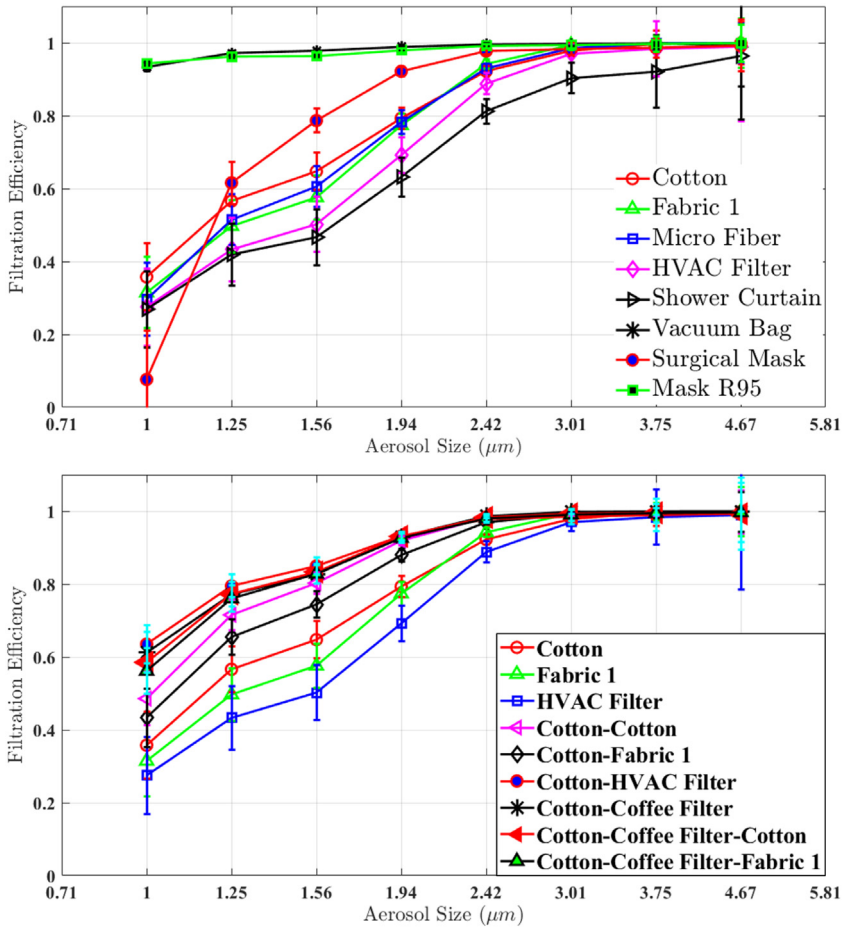

Figure 6. Filtration efficiency of tested materials, including (top) single-layer and (bottom) multiple layers, at a flow rate of 300 LPM.

4.7 μm. As well, the results indicated that large-size aerosol droplets that impinged on the tested materials, broke into smaller droplets, and passed through the layer. Single-layer materials, cotton, fabric 1, and microfiber cloth had similar filtration efficiency. Shower curtain and HVAC filter had lower efficiency for all aerosol droplets sizes, and their averaged filtration efficiency was 74.4% and 74.7%, respectively. When the materials were made of multiple layers, combining cotton, fabric 1, HVAC filter, and a coffee filter, the acquired results of filtration efficiency were found to improve for all aerosol droplet sizes. Moreover, it was found that the averaged filtration efficiency of the combined multilayer materials increased from 4% to 15% when compared to that of the single-layer materials. All tested multilayer materials had a filtration efficiency greater than 95% at the aerosol droplet size of 2.42 μm.

The pressure differences across the tested materials were also reported and can be considered for the level of comfort and breathability for homemade masks. It was found that as a single-layer material, non-woven fabric 1 had the smallest pressure difference because of its porous structure. Two-layer materials had three to four times higher pressure differences than single-layer ones. The tested two-layer materials of a cotton-HVAC filter and cotton fabric 1 had the smallest pressure differences, and similar averaged filtration efficiency of 90%. The three-layer materials, i.e., cotton-coffee filter-cotton and cotton-coffee filter-fabric 1, had a filtration efficiency higher than 90%. However, their pressure differences were found to be two to 2.5 times higher than those of two-layer materials. The tested R95 mask with five layers had a pressure difference lower than those of the two-layer materials because it was made from porous layers.

Author contributions

Blake Maher, Reynaldo Chavez, and Gabriel C. Q. Tomaz contributed equally.

Conflict of interests

The authors report no conflict of interest.

Funding source

None.

Ethical approval

Ethical approval was not required.

Acknowledgment

The experimental instrumentation used in this study was funded by the U.S. Department of Energy under an Infrastructure grant of the Nuclear Energy University Program (NEUP) for nuclear research.

References

Asadi S, Wexler AS, Cappa CD, Barreda S, Bouvier NM, Ristenpart WD. Aerosol emission and superemission during human speech increase with voice loudness. Sci Rep 2019;9(1):1–10.

Barasheed O, Alfelali M, Mushta S, Bokhary H, Alshehri J, Attar AA, et al. Uptake and effectiveness of facemask against respiratory infections at mass gatherings: a systematic review. Int J Infect Dis 2016;47:105–11.

Bourouiba L, Dehandschoewercker E, Bush JW. Violent expiratory events: on coughing and sneezing. J Fluid Mech 2014;745:537–63.

Busco G, Yang SR, Seo J, Hassan YA. Sneezing and asymptomatic virus transmission. Physics Fluids 2020;32(7)073309.

Chughtai A, MacIntyre R, Peng Y, Wang Q, Ashraf M, Dung T, et al. Infection control survey in the hospitals to examine the role of masks and respirators for the prevention of respiratory infections in healthcare workers (hcws). Int J Infect Dis 2014;21:408.

Craven BA, Settles GS. A Computational and Experimental Investigation of the Human Thermal Plume. J Fluids Eng 2006;128(6):1251–8.

Dbouk T, Drikakis D. On coughing and airborne droplet transmission to humans. Physics Fluids 2020a;32(5)053310.

Dbouk T, Drikakis D. On respiratory droplets and face masks. Physics Fluids 2020b;32(6)063303.

Duguid J. The size and the duration of air-carriage of respiratory droplets and droplet-nuclei. Epidemiol Infect 1946;44(6):471–9.

Eckstein A, Vlachos PP. Digital particle image velocimetry (dpiv) robust phase correlation. Meas Sci Technol 2009;20(5)055401.

Han Z, Weng W, Huang Q. Characterizations of particle size distribution of the droplets exhaled by sneeze. J Royal Soc Interface 2013;10(88)20130560.

Hinds WC. Aerosol Technology: Properties, Behavior, and Measurement of Airborne Particles. John Wiley & Sons; 1999.

Konda A, Prakash A, Moss GA, Schmoldt M, Grant GD, Guha S. Aerosol Filtration Efficiency of Common Fabrics used in Respiratory Cloth Masks, ACS Nano. 2020.

Kutter JS, Spronken MI, Fraaij PL, Fouchier RA, Herfst S. Transmission routes of respiratory viruses among humans. Current opin virol 2018;28:142–51.

Li Y, Leung GM, Tang J, Yang X, Chao C, Lin JZ, et al. Role of ventilation in airborne transmission of infectious agents in the built environment-a multidisciplinary systematic review. Indoor air 2007;17(1):2–18.

Licina D, Pantelic J, Melikov A, Sekhar C, Tham KW. Experimental investigation of the human convective boundary layer in a quiescent indoor environment. Build Environ 2014;75:79–91.

MacIntyre CR, Dwyer D, Seale H, Fasher M, Booy R, Cheung P, et al. The first randomized, controlled clinical trial of mask use in households to prevent respiratory virus transmission. Int J Infect Dis 2008;12(1):e328.

Milton DK, Fabian MP, Cowling BJ, Grantham ML, McDevitt JJ. Influenza virus aerosols in human exhaled breath: particle size, culturability, and effect of surgical masks. PLoS pathogens 2013;9(3).

Mittal R, Ni R, Seo JH. The flow physics of covid-19. J Fluid Mech 2020;894:F2.

Morawska L, Johnson G, Ristovski Z, Hargreaves M, Mengersen K, Corbett S, et al. Size distribution and sites of origin of droplets expelled from the human respiratory tract during expiratory activities. J Aerosol Sci 2009;40(3):256–69.

Nguyen T, Goth N, Jones P, Lee S, Vaghetto R, Hassan Y. PIV measurements of turbulent flows in a 61-pin wire-wrapped hexagonal fuel bundle. Int J Heat Fluid Flow 2017;65:47–59.

Nguyen T, Goth N, Jones P, Vaghetto R, Hassan Y. Stereoscopic piv measurements of near-wall flow in a tightly packed rod bundle with wire spacers. Exp Thermal Fluid Sci 2018a;92:420–35.

Nguyen T, Hassan Y. Stereoscopic particle image velocimetry measurements of flow in a rod bundle with a spacer grid and mixing vanes at a low Reynolds number. Int J Heat Fluid Flow 2017;67:202–19.

Nguyen T, Kappes E, King S, Hassan Y, Ugaz V. Time-resolved PIV measurements in a low-aspect ratio facility of randomly packed spheres and flow analysis using modal decomposition. Exp Fluids 2018b;59(8):127.

Nguyen T, Maher B, Hassan Y. Flow-field characteristics of a supersonic jet impinging on an inclined surface. AIAA J 2019a;1–15.

Nguyen T, Muyshondt R, Hassan Y, Anand N. Experimental investigation of cross flow mixing in a randomly packed bed and streamwise vortex characteristics using particle image velocimetry and proper orthogonal decomposition analysis. Physics Fluids 2019b;31(2)025101.

Nguyen T, Vaghetto R, Hassan Y. Experimental investigation of turbulent wake flows in a helically wrapped rod bundle in presence of localized blockages. Physics Fluids 2020;32(7)075113.

Nguyen T, White L, Vaghetto R, Hassan Y. Turbulent flow and vortex characteristics in a blocked subchannel of a helically wrapped rod bundle. Exp Fluids 2019c;60(8):129.

Offeddua V, Yungb C, Lowc M, Tamd C. Effectiveness of masks and respirators against respiratory infections in healthcare workers: A systematic review and meta-analysis. Int J Infect Dis 2016;4(163):163.

Rostami AA. Computational modeling of aerosol deposition in respiratory tract: a review. Inhalation toxicol 2009;21(4):262–90.

Scharfman B, Techet A, Bush J, Bourouiba L. Visualization of sneeze ejecta: steps of fluid fragmentation leading to respiratory droplets. Exp Fluids 2016;57(2):24.

Shakya KM, Noyes A, Kallin R, Peltier RE. Evaluating the efficacy of cloth facemasks in reducing particulate matter exposure. J Exposure Sci Environ Epidemiol 2017;27(3):352–7.

Stelzer-Braid S, Oliver BG, Blazey AJ, Argent E, Newsome TP, Rawlinson WD, et al. Exhalation of respiratory viruses by breathing, coughing, and talking. J Med Virol 2009;81(9):1674–9.

Tang J, Li Y, Eames I, Chan P, Ridgway G. Factors involved in the aerosol transmission of infection and control of ventilation in healthcare premises. J Hospital Infect 2006;64(2):100–14.

Vincent JH. Aerosol Sampling: Science, Standards, Instrumentation and Applications. John Wiley & Sons; 2007.

Wells W. On airborne infection: Study ii. droplets and droplet nuclei. Am J Epidemiol 1934;20(3):611–8.

Wells WF. Airborne contagion and air hygiene. An ecological study of droplet infections. J Am Med Assoc 1955;190(1).

Xie X, Li Y, Sun H, Liu L. Exhaled droplets due to talking and coughing. J Royal Soc Interface 2009;6(suppl_6):S703–14.